Journal of Sol-Gel Science and Technology 27, 343–354, 2003

Structural Control in Poly(butyl acrylate)-Silica Hybrids by Modifying Polymer-Silica Interactions

RICARDO O.R. COSTA AND FERNANDO S. LAMEIRAS
Centro de Desenvolvimento da Tecnologia Nuclear—CDTN/CNEN, Belo Horizonte, 30123-970, Brazil

WANDER L. VASCONCELOS*
Departamento de Engenharia Metalúrgica e de Materiais, Universidade Federal de Minas Gerais, Rua Espírito Santo, 35, Belo Horizonte, MG, Brazil 30160-030
wlv@demet.ufmg.br

Received July 2, 2002; Accepted October 28, 2002

Abstract. Porous organic-inorganic hybrids of poly(n-butyl acrylate) (PBA) and silica were synthesized with different polymer contents via sol-gel process. With the aim of controlling interfacial properties in hybrids, the bonding agent 3-methacryloxypropyl-trimethoxysilane (MPTS) was copolymerized with n-butyl acrylate (BA) at different proportions. Copolymers P(BA-co-MPTS) and hybrids obtained were characterized by infrared spectroscopy and thermogravimetric analysis. Nitrogen sorption analyses of hybrids determined that the increase in polymer content leads to the formation of non-porous hybrids only if bonding agent content is sufficiently large. Otherwise, hybrids with large pore volumes and sizes, nearly reaching macropore range, are obtained even for polymer content as high as 45% in the absence or low content of MPTS. Scanning electron microscopy images showed that the addition of bonding agent changes the aspect of hybrid surface from rough, with loosely bound particles with a few hundreds nanometers, to relatively smooth, with particles typically smaller than 100 nm. These results were explained considering that a more homogeneous medium provided by the presence of MPTS may lead to easier condensation of PBA-silica particles due to the smaller polymeric domains. This idea is supported by the fact that, after polymer degradation, smaller uniform-sized pores arise for hybrids with larger bonding agent contents.

Keywords: organic-inorganic hybrid, pore structure, poly(butyl acrylate), sol-gel

1. Introduction

Over the past two decades, there has been an increasing interest in the study of organic-inorganic hybrid materials by industrial and academic groups [1] due to their potential applications and the possibility to control synthesis-structure-property relationships. The synthesis of sol-gel derived hybrids is particularly attractive because of the simplicity and versatility associated with sol-gel process, which allows the easy incorporation of an organic component into a ceramic network under mild conditions [2]. Since the mid-1980s, when the first sol-gel derived hybrids were obtained by mixing linear polymer chains with silica precursors [3–5], a considerably large number of studies have been devoted to the determination of structure and properties of the resulting hybrids, as demonstrated by several reviews on this matter [6–12].

Given the facts that porosity is an intrinsic element to deal with in materials obtained via sol-gel process, and that the incorporation of organic components to these materials may constitute an important tool to provide access to structural control, the study of pore structure in sol-gel derived organic-inorganic hybrids becomes

*To whom all correspondence should be addressed.

inevitable. Additionally, the interest in potential technological applications such as catalyst supports, separations media, sensors, etc, led to the development of techniques for synthesis of porous materials with controlled pore size distributions, particularly involving organic templating methods [13–17].

A wide variety of types of organic polymers have been employed in the syntheses of hybrids [8, 9], especially of silica. The type of polymer employed is one of the main features affecting microstructure and macroscopic characteristics of hybrids because they depend essentially on chemical interactions established between organic and inorganic moieties. More specifically, polymer content and its molecular weight [9], the presence, size and type of pendant groups, the insertion and concentration of Si─C covalent bonds either at the end or in the middle of polymeric chains [6, 9–11]; each one of these features may affect structure considerably, leading to transparent or opaque, rigid or flexible, porous or non-porous materials.

Poly(butyl acrylate) (PBA) is an attractive polymer for these studies due to its low glass transition temperature, which in principle might confer flexibility to hybrid materials. However, PBA exhibits poor interactions with hydroxy groups generated by sol-gel reactions because of the rather hydrophobic nature of butyl side groups. This is demonstrated by the formation of a 2-phase PBA-titania hybrid produced by Mauritz and Jones [18], and by the necessity of copolymerization of butyl acrylate [19, 20] or butyl methacrylate [21] with more hydrophilic monomers or bonding agents to produce homogenous hybrids. Despite the difficulty associated with structural heterogeneity, poor PBA-silica interactions might be explored as a tool for structural control if a reverse tool such as a bonding agent addition is employed. Investigations of the influence of bonding agent content on thermal and macroscopic properties of hybrids have been carried out [20, 21], but attention has been focused on high polymer concentration systems. Therefore, non-porous hybrids are mostly obtained and information on pore structure of PBA-silica system becomes unavailable.

This paper aims to change the nature of PBA-silica interactions in porous hybrids within a range of compositions by copolymerization of butyl acrylate with the bonding agent 3-methacryloxypropyl-trimethoxysilane (MPTS) at different proportions. The main objective was to evaluate the influence of the primary bonds formed between organic and inorganic moieties on structure of hybrids.

2. Experimental

The syntheses of PBA-silica hybrids followed a 2-step procedure. In a first step the monomer n-butyl acrylate (BA) was either polymerized to form PBA or copolymerized with the bonding agent 3-methacryloxypropyl-trimethoxysilane (MPTS) to form different copolymers P(BA-co-MPTS), namely PBMTy, where "y" is equal to 1, 5, 10 and 20, and corresponds to the number of moles of MPTS added for each 100 moles of BA in the monomer solution. In a following step, polymer solutions were employed along with silica precursors to produce hybrids TxB (without bonding agent), obtained using the homopolymer PBA, and hybrids TxBMTy, obtained from copolymers PBMTy. In both cases, "x" means the ratio of tetramethoxysilane (TMOS) volume (mL) to PBA mass (g) and the values selected were 9, 6, 4, 3 and 2. Therefore, a decreasing "x" corresponds to an increasing amount of the organic moiety in the hybrid. A larger "y" corresponds to an increase in the probability of formation of covalent bonds between polymer chains and silica network due to the higher concentration of bonding agent. The following sections describe a typical synthesis procedure. Unless otherwise noted, reagents were used as received.

2.1. Syntheses of PBA and P(BA-co-MPTS)

PBA was synthesized under N_2 by dissolving 3.00 mL (20.9 mmol) of the monomer BA (98% Polysciences) and 0,00375 g (0.0228 mmol) of the initiator 2,2'-azobis(isobutyronitrile) (AIBN) (98% Aldrich) in 6.0 mL of 1-butanol (99.5% Merck). The sealed reacting flask was heated to $(70 \pm 1)^{\circ}$C for 24 h. The resulting polymer solution was directly employed for the syntheses of hybrids TxB. The syntheses of PBMT1, PBMT5, PBMT10 and PBMT20 followed a similar procedure, but with addition of 0.050 mL (0.209 mmol), 0.250 mL (1.05 mmol), 0.500 mL (2.09 mmol) and 1.00 mL (4.18 mmol) of MPTS (98% Polysciences), respectively, together with BA and AIBN. To obtain PBMT20, the monomer solution had to be diluted using 12.0 mL of 1-butanol instead of 6.0 mL to avoid gelation of polymer solution. The PBMTy solutions were directly employed to produce hybrids TxBMTy. It was determined by gravimetric measurements before and after drying that conversions higher than 90% were attained.

Table 1. Reaction conditions for the syntheses of hybrids TxB and TxBMTy from polymer solutions.

	T9B/ T9BMTy[a]	T6B/ T6BMTy	T4B/ T4BMTy	T3B/ T3BMTy	T2B/ T2BMTy
Polymer solution (g)	0.308	0.462	0.694	0.926	1.328
Additional amount of 1-butanol (mL)[b]	1.76	1.64	1.45	1.27	0.90
Solution TMOS—methanol—H_2O (mL)	2.04	2.04	2.04	2.04	2.04
Ratio x = TMOS(mL)/polymer(g)[c]	9	6	4	3	2
Nominal % polymer[d]	21.6	29.1	38.2	45.2	55.3

[a] *y* is equal to 1, 5, 10, 20, which correspond to the number of moles of MPTS added for each 100 moles of BA in the monomer solution.
[b] Total amount of 1-butanol was ∼2.0 mL in each reacting solution. To produce hybrids TxBMT20 volumes added were 1.64, 1.47, 1.19, 0.93 and 0.39 mL, respectively.
[c] Expected ratio, calculations not shown.
[d] Theoretical polymer contents expected, calculated considering only PBA and dry silica, assuming total conversion of TMOS into SiO_2, without remaining free water molecules, silanol or alcoxide groups. 1.00 g of TMOS is theoretically converted to 0.3047 g of SiO_2.

2.2. *Syntheses of Hybrids TxB and TxBMTy*

The direct use of polymer solutions to produce hybrids TxB and TxBMT, instead of obtaining the dried polymer, aims both to simplify the procedure and to avoid the exposure of alkoxide groups of bonding agent to moisture of air, thus minimizing the risk of premature hydrolysis. The desired amounts of polymer solution (Table 1) were weighed in 13 mL cylindrical flasks and specific volumes of 1-butanol were added, so as to equalize the volume of solvent present in all flasks, nominally ∼2.0 mL. The volumes were calculated based on the estimated amount of 1-butanol in the polymer solutions considering 100% conversion and no losses. In another flask, 10.0 mL of distilled and deionized water, 12.0 mL of methanol (99.5% Merck) and 20.0 mL of TMOS (98% Aldrich) were added under magnetic stirring. The flask was closed to avoid losses and the stirring was maintained for more 10 min. Then, 2.04 mL of this solution were added to each one of those flasks containing the polymer solutions previously diluted with 1-butanol. This amount corresponds roughly to 1.0 mL of TMOS, 0.5 mL of water and 0.6 mL of methanol, if added separately. The flasks were then sealed and maintained at room temperature. Gelation took place after 2–3 days, depending on the composition. Samples were aged during ∼3 days at room temperature and 40 h at 60°C. Samples were then dried for 24 h at 50°C, 24 h at 80°C and 36 h at 120°C. Disc-shaped solids were obtained with various diameters and thickness, depending on the composition, and kept in sealed flasks until measured.

Table 1 presents the amounts of reagents employed to synthesize hybrids TxB and TxBMTy, where "x" values (TMOS:PBA ratios) correspond to 9, 6, 4, 3 and 2, giving hybrids with nominal polymer contents of 21.6, 29.1, 38.2, 45.2, 55.3 wt%, respectively. The nominal contents were calculated considering only polymer and dry silica, assuming total conversion of TMOS into SiO_2.

Silica was also synthesized without addition of organic polymer and characterized in the same way as hybrids. The procedure followed was the same, using 1.0 mL of TMOS, 0.5 mL of water, 0.6 mL of methanol and 2.0 mL of 1-butanol, since the idea was to evaluate only the effect of polymer addition. Another type of silica named "silica B" was obtained from the mixture without addition of 1-butanol, so as to evaluate the effect of solvent individually.

2.3. *Properties*

PBA and P(BA-co-MPTS) were analyzed by Fourier transform infrared spectroscopy (FTIR) (Perkin Elmer FT-IR Spectrometer Spectrum 1000). Polymer solutions were poured into a large excess of methanol under magnetic stirring to precipitate the polymer and copolymer, which were then dried at 70°C. An Attenuated Total Reflexion (ATR) apparatus was employed for measuring the spectra, with at least 16 scans at a resolution of 2 cm^{-1}. Hybrids were crushed into fine powder and analyzed using a diffuse reflectance apparatus, with small amounts of sample placed on an aluminum-coated abrasive pad.

Nitrogen sorption analyses (Quantachrome Autosorb-1) of the obtained hybrids were performed by crushing the samples into small pieces (<1 mm)

and degassing at 120°C for at least 12 h. Surface areas were calculated using Brunauer-Emett-Teller (BET) equation [22] with 5 adsorption points. Pore size distributions were calculated from desorption branches of isotherms using the method proposed by Barret, Joyner and Halenda (BJH) [23]. Selected samples were heat treated to 600°C for 1 h to burn out the organic moieties and then submitted to analyses by N_2 sorption.

Thermogravimetric analyses (TGA) of hybrids were conducted (Shimadzu TGA-50) by heating ∼8 mg of powdered samples to 900°C at 20°C/min with a flow of 20 mL N_2/min. Scanning electron microscopy (SEM) images of hybrids were obtained on a JEOL JSM-840A.

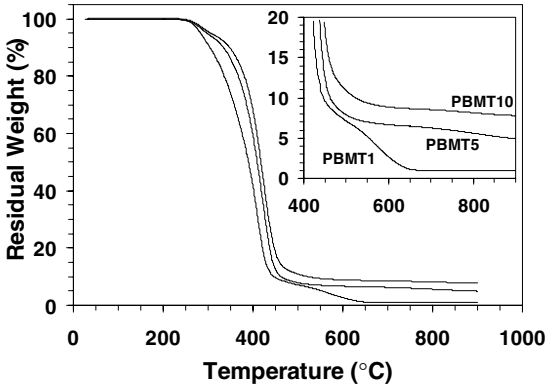

Figure 2. TG curves for copolymers PBMT1, PBMT5 and PBMT10.

3. Results and Discussion

3.1. Syntheses of PBA and P(BA-co-MPTS)

FTIR spectra for the obtained polymer PBA and copolymers PBMT1, PBMT5, PBMT10 and PBMT20 are compared in Fig. 1. Spectrum (a) exhibits typical absorption bands of PBA, including a strong peak at 1720 cm^{-1}, assigned to C═O [24–26], and the relatively broad peak in the region 2800–3000 cm^{-1} corresponding to C─H vibrations of PBA backbone and side groups. The main features observed at the spectra of the copolymers (Figs. 1(b)–(e)) are the occurrence of progressively stronger peaks at 1085 and 820 cm^{-1}, which may be assigned to Si─O─C bending [26, 27] and Si─C stretching vibration [26, 28], respectively. Also with increasing MPTS:BA mol ratio, it arises a small peak at 2840 cm^{-1} related to C─H stretching of methoxy groups belonging to the bonding agent MPTS copolymerized with BA [26, 27].

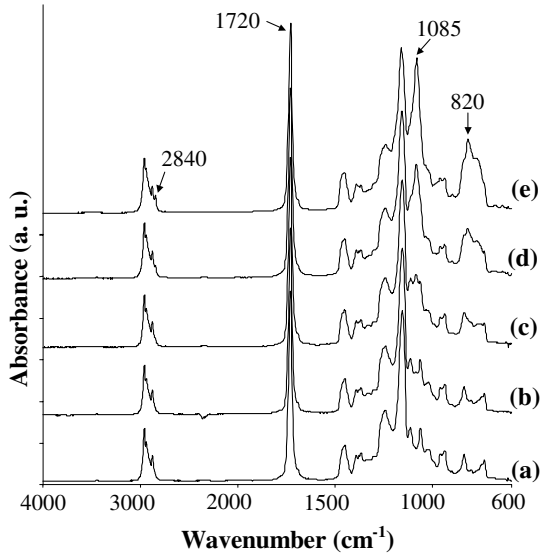

Figure 1. FTIR spectra of polymer PBA (a) and copolymers PBMT1 (b), PBMT5 (c), PBMT10 (d) and PBMT20 (e).

Figure 2 shows the weight loss curves obtained from TGA measurements of the copolymers PBMT1, PBMT5 and PBMT10. The similar weight loss profile and the increasing residual weight at 900°C (in detail) confirm the copolymerization of BA with larger amounts of MPTS, since the Si─(OCH_3) groups may be at least partially transformed into SiO_2.

3.2. Syntheses of Hybrids TxB and TxBMTy

Figure 3 exhibits FTIR spectra for silica, silica B (without 1-butanol), and hybrid T4BMT10. It can be observed that the spectrum of silica (Fig. 3(b)) presents peaks at 1382 cm^{-1}, 1453 cm^{-1}, 2868 cm^{-1} and 2953 cm^{-1}, which may be assigned to the residual 1-butanol, a less volatile alcohol (bp = 118°C), and to not condensed Si─OBu groups generated from substitution of Si─OMe groups during hydrolysis [29]. The structural consequences of this feature will be discussed later in the light of nitrogen sorption results and SEM images. The spectrum (c) in Fig. 3 is typical for the hybrids produced and confirms the incorporation of PBA due to the presence of the intense C═O peak at 1723 cm^{-1}, comparatively with the H_2O peak at 1630 cm^{-1}. The peaks at 1382 cm^{-1}, 1453 cm^{-1}, 2868 cm^{-1} and 2953 cm^{-1} larger than in pure silica,

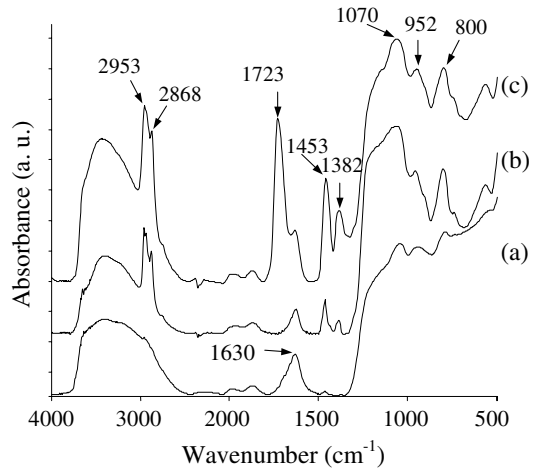

Figure 3. FTIR spectra of silica B (a), silica (b) and hybrid T4BMT10 (c).

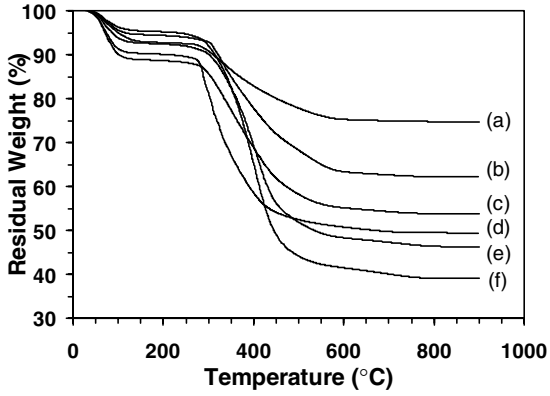

Figure 4. TG curves for silica (a) and hybrids T9BMT10 (b), T6BMT10 (c), T4BMT10 (d), T3BMT10 (e) and T2BMT10 (f).

although might suggest the presence of 1-butanol, may also be assigned to C—H bonds of polymer groups. The other absorption peaks of polymer are hidden in the spectrum of hybrids by the larger amplitude peaks of silica gel in the region 800–1200 cm^{-1}.

The TGA results are presented in Fig. 4 for silica and hybrids TxBMT10. The weight loss in 2 steps corresponds to the evaporation of non-bonded water and other volatile compounds (<200°C) and to polymer degradation overlapped with loss of silica gel bonded groups such as —OH and non-hydrolyzed $—OCH_3$ (200°C < T < 900°C). Although it is not possible to resolve these 2 contributions, TGA data confirm that the total weight loss increases with nominal polymer content (cf. Table 1). It is interesting that the weight loss concerning volatile compounds seems to be higher for intermediate polymer contents T6BMT10 (Fig. 4(c)) and T4BMT10 (Fig. 4(d)) than for silica, which might be related somehow to the differences in pore structure of materials.

3.3. *Textural Properties*

From N_2 sorption analyses of silica and hybrids, it was obtained pore surface areas (S_p) and specific pore volumes (V_p), which are presented in Figs. 5 and 6, respectively. In a general way, it is observed a decrease in both S_p and V_p for all types of hybrids with increasing PBA content probably due to a pore filling effect. However, while there is no substantial difference in S_p of hybrids with various amounts of bonding agent, attention must

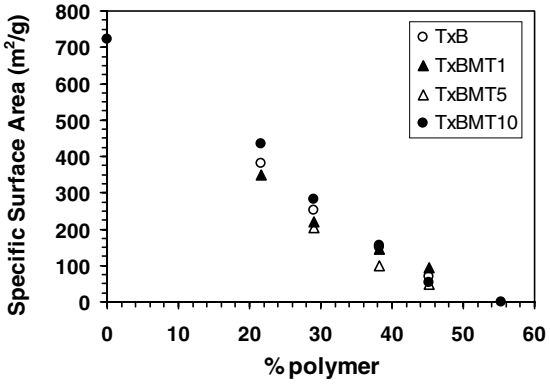

Figure 5. Dependence of specific pore surface area on nominal polymer content in hybrids TxB, TxBMT1, TxBMT5 and TxBMT10. Errors are within 5%.

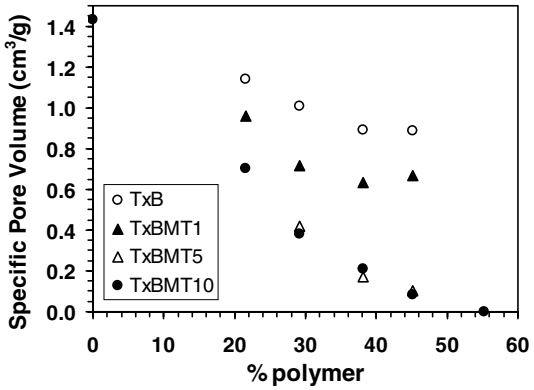

Figure 6. Dependence of specific pore volume on nominal polymer content in hybrids TxB, TxBMT1, TxBMT5 and TxBMT10. Errors are within 5%.

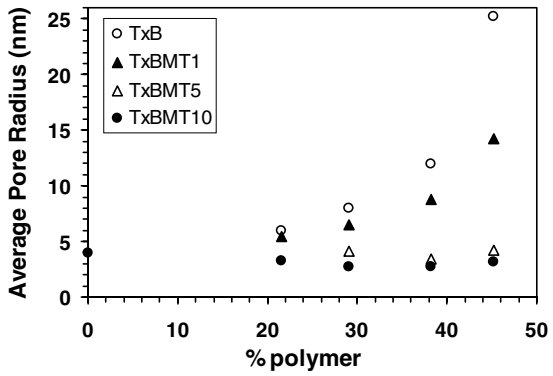

Figure 7. Dependence of pore radius on nominal polymer content in hybrids TxB, TxBMT1, TxBMT5 and TxBMT10. Errors are within 7%.

be drawn to the strong dependence of V_p on MPTS content. The addition of ∼50% polymer leads to the formation of hybrids TxBMT10 and TxBMT5 essentially non-porous (Fig. 6), but a different behavior is observed in hybrids TxB and TxBMT1, for which the absence or low content of bonding agent leads to materials with large porosities even for PBA content as high as 45%.

In the same way, the average pore radius (R_p) of hybrids is strongly affected by MPTS content, as demonstrated in Fig. 7. While the increase in polymer content keeps pore size within the range 2.7 nm $< R_p <$ 4.2 nm (small mesopores) in hybrids TxBMT5 and TxBMT10, the absence of bonding agent in hybrids TxB leads to the formation of materials with R_p as high as 25 nm, reaching the lower macropore range (50 nm in diameter).

The reasons for the continuous decrease in V_p and R_p with the addition of progressively larger amounts of bonding agent are related to the change of interactions between polymer and silica network. The poor interactions between hydrophobic PBA chains and Si—OH groups in hybrids TxB make more difficult the condensation between silica particles, thus leading to a less integrated network. When the bonding agent is introduced, even though PBA segments may still promote steric hindrance to some extent, covalent bonds formed between polymer chains and silica particles may contribute for the integrity of silica network as well as for the formation of a hybrid with the organic moiety more equally dispersed throughout the structure. Similar but not so dramatic differences have already been found by our group for poly(2-hydroxyethyl methacrylate)-silica hybrids [30].

3.4. SEM Images

The influence of MPTS content on the integrity of silica network can be more profoundly discussed with the aid of SEM images presented in Fig. 8. Micrograph (a) represents a fracture surface of the obtained silica, where it is possible to distinguish many condensed silica particles with a few hundreds nanometers, some of them even reaching 1 μm in size. The relatively smooth surface differs from what is seen at micrograph (b), which represents surface of hybrid T3B. In this case, the rougher surface with loosely bound particles demonstrates that, even though similar condensation mechanisms might be involved, the incorporation of PBA chains tends to hinder condensation of Si—OH groups. Because of the inefficient packing of hybrid particles, highly porous materials are formed with pores larger than micro and mesopores typically encountered in silica network (Fig. 7).

The addition of bonding agent changes completely the aspect of surface of hybrid T3BMT10, as noted in Fig. 8(c). With the same magnification (10,000×), it is nearly impossible to distinguish particles, which are typically less than 100 nm in size. The smooth surface is in agreement with the structure determined by N_2 sorption analysis (Figs. 6 and 7), which contains low pore volume and size. The small particle size likely results from higher condensation rates, given that the bonding agent may lead to a more profound interpenetration of polymer chains within silica network.

Figure 8(d) is an image of a typical surface of silica B (without 1-butanol). The smoother surface obtained, with smaller and well-packed particles comparatively with Fig. 8(a), indicates that condensation is favored in absence of 1-butanol. The main difference caused by the presence of 1-butanol is the substitution of Si—OMe groups with Si—OBu groups, leading to a lower hydrolysis rate [29]. As pointed out earlier, the FTIR spectrum of silica (Fig. 3(b)) shows peaks, assigned to remaining Si—OBu groups not condensed, that are absent in spectrum of silica B (Fig. 3(a)). Therefore, the use of methanol as the single solvent leads to a more condensed silica network, as confirmed by the decrease in V_p and R_p from 1.43 cm^3/g and 4.0 nm for silica, to 0.56 cm^3/g and 1.5 nm for silica B, respectively. The difference between textural properties of silica and silica B can be illustrated by comparing their sorption isotherms in Fig. 9, where a smaller hysteresis loop shifted to lower relative pressures indicates the occurrence of smaller pores in absence of 1-butanol. Besides

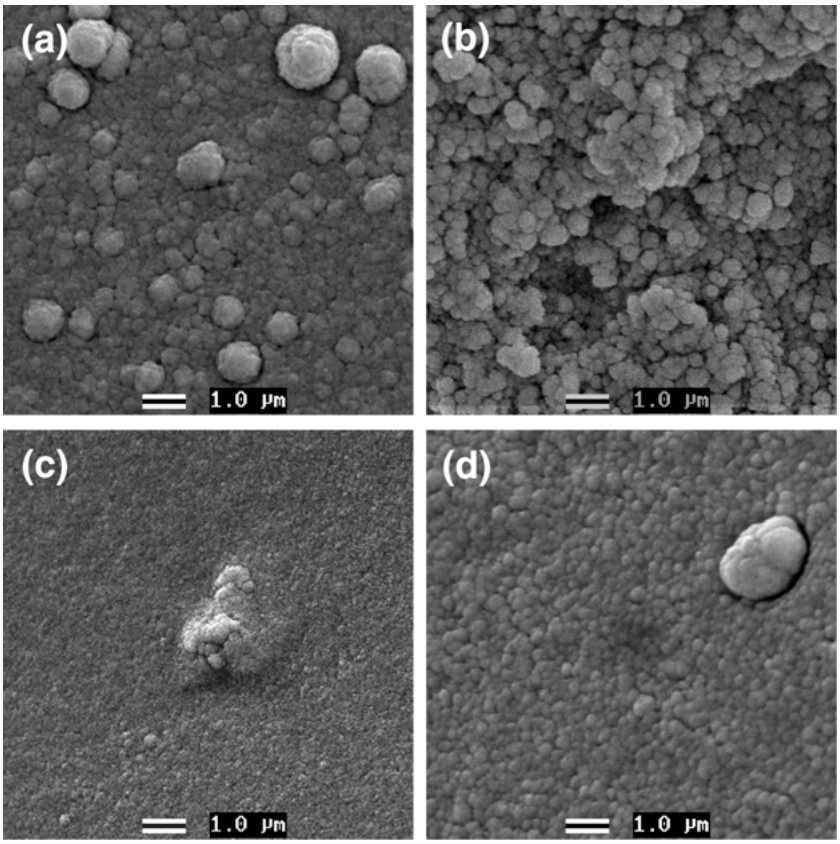

Figure 8. SEM images (10,000×) of fractured surfaces of silica (a), hybrid T3B (b), hybrid T3BMT10 (c) and silica B (d).

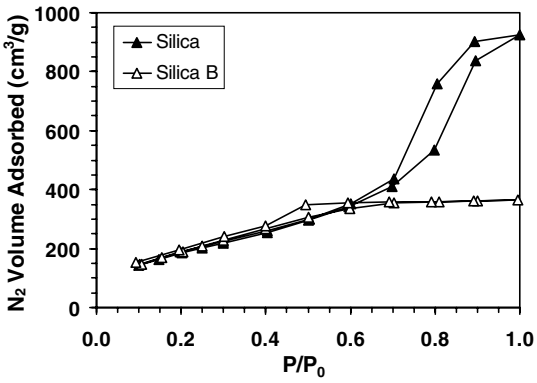

Figure 9. Nitrogen adsorption-desorption isotherms of silica and silica B (without 1-butanol) at 77 K.

the considerations involving the presence of Si─OBu groups, the lower contact angle between methanol and silica would lead to a larger heat of wetting or capillary stress, thus favoring condensation reactions [2], which might also contribute for the lower pore volume and size observed in absence of 1-butanol.

In Fig. 10, SEM images of hybrids TxBMT1 (a) and TxBMT5 (b) with a larger magnification (50,000×) are compared. The previous observation is confirmed, i.e., the hybrid with less bonding agent has a rougher surface with larger particles, which originate its larger pore volume and size (Figs. 6 and 7). It is important to point out that, although the magnification is not large enough to identify average pore sizes as small as 10 nm, the previous discussion is still reasonable if one considers the fractal nature of these materials. In other words, the aspects observed concerning the larger distinguishable particles simply result from the configuration assumed by their elementary particles, which are, in turn, affected by issues like the hindrance of PBA segments to Si─OH condensation and covalent bonds formed between polymer chains and silica. The inefficient packing of elementary hybrid particles is responsible for a similarly disordered packing of the

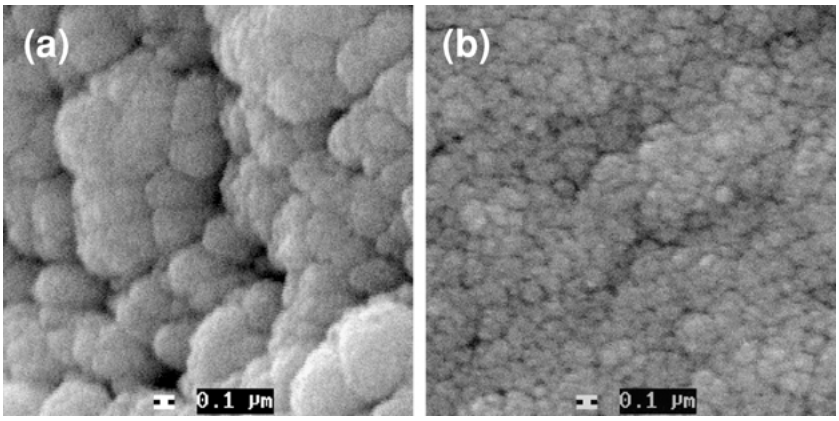

Figure 10. SEM images (50,000×) of fractured surfaces of hybrids T3BMT1 (a) and T3BMT5 (b).

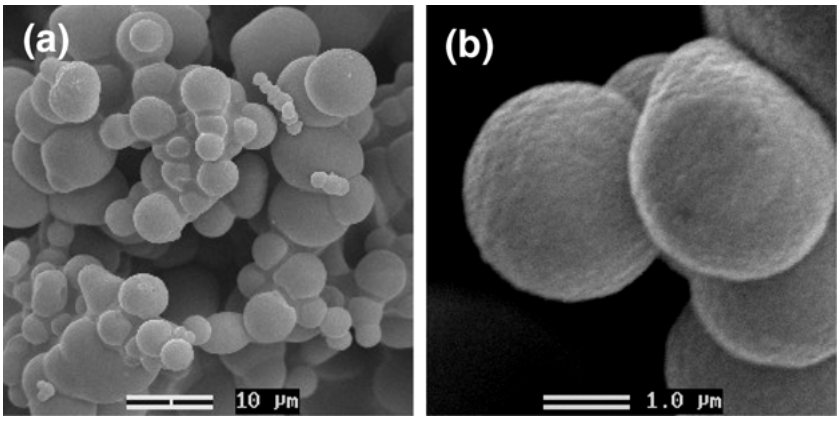

Figure 11. SEM images of hybrid T2B (powder) with magnifications of 2,000× (a) and 20,000× (b).

larger particles, thus generating the structures observed at lower magnifications.

To stress the significance of PBA segments on hindrance to Si─OH condensation, SEM images of hybrid T2B are shown in Fig. 11. Because of the large PBA content (∼55%) and absence of bonding agent, there was phase separation and it was not possible to obtain a monolith. As it can be observed, the obtained powder is formed by large smooth round particles, ranging from 1 μm to several microns. On the other hand, hybrid T2BMT10 was obtained as an essentially non-porous (Fig. 6) monolith. The differences observed between T2B (Fig. 11) and T3B (Fig. 8(b)) structures also support the previous arguments that the increase in PBA content makes condensation more difficult, unless a minimum amount of bonding agent is added.

3.5. Pore Size Distributions

It has been shown that pore volume and size of hybrids are strongly affected by polymer and bonding agent contents. Figures 12 and 13 show N_2 adsorption-desorption isotherms for some of the hybrids TxB and TXBMT10, respectively, comparatively to silica. The decrease in total N_2 volume adsorbed with increasing polymer content is evident for both types of hybrids, which has already been demonstrated in Fig. 6. The interesting point to be observed is the shift of the hysteresis loop to the right for hybrids TxB (Fig. 12) and to the left for hybrids TxBMT10 (Fig. 13). This indicates a tendency for increasing pore size of hybrids TxB (cf. Fig. 7) and for decreasing pore size of hybrids TxBMT10, which is not perfectly clear by just looking at Fig. 7. This observation reveals that the addition of

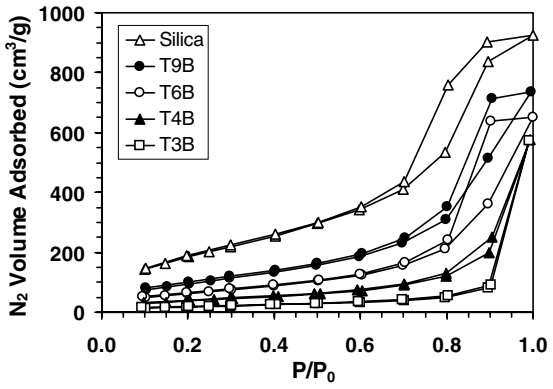

Figure 12. Nitrogen adsorption-desorption isotherms of silica and hybrids TxB at 77 K.

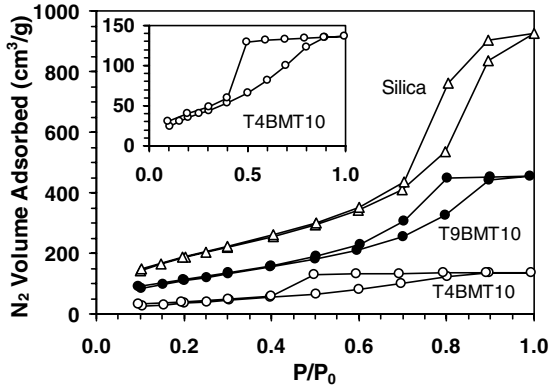

Figure 13. Nitrogen adsorption-desorption isotherms of silica and hybrids T9BMT10 and T4BMT10 at 77 K.

bonding agent changes significantly the PBA-silica interactions, so as to nearly annul hindrance promoted by PBA segments. Another complementary observation in Fig. 12 is that isotherms of hybrids T4B and T3B are of type III, according to Brunauer's classification [22], suggesting that pore volumes are not satisfactorily measured by N_2 sorption technique due to larger pore sizes in the macropore range. Therefore, R_p values experimentally determined for hybrids T4B and T3B may be used as reference, but the real values are probably even larger than the ones plotted in Fig. 7.

A very interesting observation is that polymer and bonding agent contents affect not only the average pore sizes but also pore size distributions. According to Fig. 14, the considerably broad pore size distribution of silica is progressively narrowed in hybrids TxBMT10 as polymer content is increased. Hybrid T4BMT10 has a very narrow pore radius distribution centered

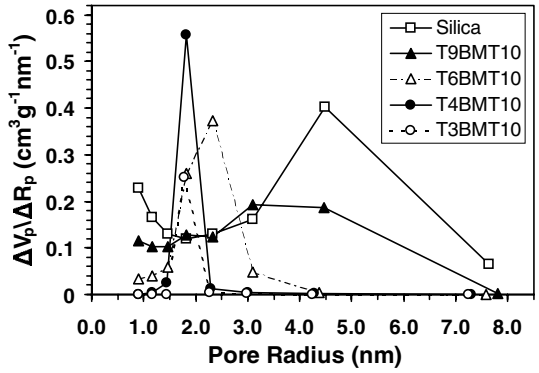

Figure 14. Comparison of pore radius distributions in silica and hybrids TxBMT10 with increasing polymer content.

at 1.8 nm and a similar behavior occurs for hybrid T3BMT10, but with a lower pore volume. It should be taken into account, however, that these distributions are based on the desorption branches of the isotherms. The hysteresis loop (detail in Fig. 13) seems to be of type E (deBoer) or H_2 (IUPAC) [22], which is indicative of ink bottle pores. Since the adsorption branch is not as steep as the desorption branch, the distribution profiles vary considerably. On the basis of that model, the narrow distribution determined from desorption branch corresponds to the throat size, while the broad distribution determined from adsorption branch corresponds to the cavity size [2]. This very narrow throat size distribution may be useful for technological applications such as catalysts, molecular sieves, sensors and other purposes that require molecular selectivity by size.

In a similar manner, Fig. 15 demonstrates that the addition of bonding agent contributes to progressively

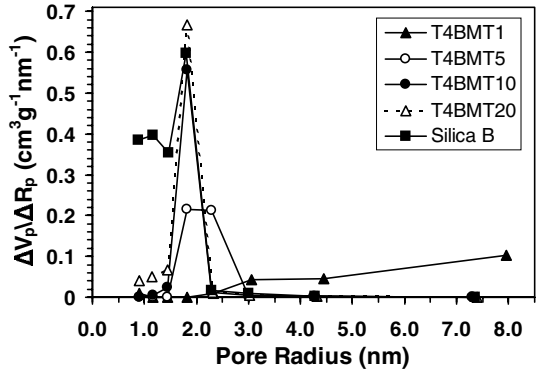

Figure 15. Comparison of pore radius distributions in silica B and hybrids T4BMTy with increasing bonding agent content.

narrow throat size distribution. The distribution is the broadest for hybrid T4B (not shown), transitional for hybrid T4BMT5 and very narrow for hybrids T4BMT10 and T4BMT20. Interestingly the peak of the narrow distributions coincides with the peak for silica B (synthesized without 1-butanol).

The occurrence of a very narrow distribution centered at 1.8 nm (Figs. 14 and 15) may be essentially interpreted as the absence of micropores and larger mesopores. The absence of micropores simply derives from the fact that they are either filled with or obstructed by polymer chains in hybrids, independently of bonding agent content (Fig. 15). The absence of larger mesopores, however, seems to be dependent on the homogeneity of hybrid structure. In a homogeneous system, polymer chains and solvent molecules are dispersed among silica nanoparticles. When these particles start to agglomerate and to form the silica network, solvent and other volatile molecules are easily excluded to the regions that will constitute the pore structure after drying. It is likely that the unfavorable interactions between the n-butyl side groups of polymer and Si–OH groups of silica lead to larger compositional fluctuation in hybrids with less bonding agent, say T4BMT1, which would ultimately foment the generation of larger polymeric domains in the final structure. As long as polymer and solvent are sufficiently compatible, larger polymeric domains would probably be accompanied by the local presence of larger amounts of solvent, thus explaining the existence of larger pore sizes. Nevertheless, in hybrids with a larger bonding agent content, say T4BMT10, polymer molecules are more likely to be equally distributed in the silica network due to the formation of primary bonds involving the linear chains and the network structure. Therefore, the formation of small polymeric domains becomes more plausible and, for an analogous reasoning to the one described above, the local presence of smaller amounts of solvent would explain the absence of larger mesopores (Fig. 15).

3.6. *Controlling Pore Structure by Changing Volume of Solvent*

The ideas exposed in last paragraph are focused on the improvement of the homogeneity of hybrid structure by adding progressively larger bonding agent contents. Another way of improving the homogeneity of hybrid structure would be to increase amounts of solvent added, whose purpose is to provide a compatible media for reactions to take place. The idea of this topic is to verify if the reduction of solvent volumes would modify pore structure in a similar manner as when bonding agent content was decreased.

The additional amounts of 1-butanol used in the syntheses of hybrids (Table 1) were previously selected so as to ensure the formation of homogeneous reacting solutions and transparent gels. However, it was possible to reduce the volume of solvent added still avoiding phase separation before gelation. A variant termed hybrid T6BMT10A was produced by adding 1.20 mL of 1-butanol instead of the 1.64 mL used for hybrid T6BMT10. A second variant termed hybrid T6BMT10B was produced with 1.00 mL of 1-butanol, but in this case heating to 50°C was necessary to obtain a homogeneous solution, which, after gelled, turned into a slightly turbid gel.

In Fig. 16 the average pore radii of hybrids are plotted as a function of either the solvent or bonding agent contents, in arbitrary units. It can be seen that pore sizes increase with reduction of 1-butanol volume (T6BMT10A and T6BMT10B) in a similar way that happens when bonding agent content is reduced (T6BMT10 to T6B). An increase in pore volumes (numbers) is also observed in both cases. Therefore, these data support the previous hypothesis that pore volume (Fig. 6) and pore size (Fig. 7) of hybrids with larger bonding agent contents decrease due to the formation of a more homogeneous hybrid structure, where condensation reactions between silica particles are favored.

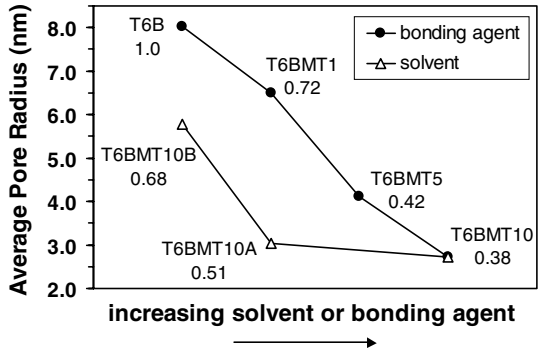

Figure 16. Comparison of average pore radius of hybrids produced by increasing 1-butanol volume from 1.00 mL (T6BMT10B) to 1.20 mL (T6BMT10A) and 1.64 mL (T6BMT10) with average pore radius of hybrids T6BMTy with increasing bonding agent content. Errors are within 7%.

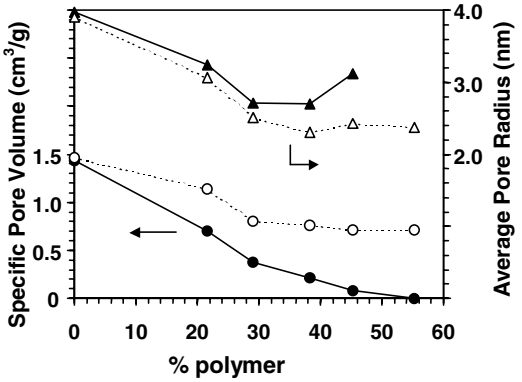

Figure 17. Pore volumes and radii in silica and hybrids TxBMT10 before (filled symbols) and after (open symbols) polymer degradation at 600°C. Errors are within 5% for V_p and 7% for R_p.

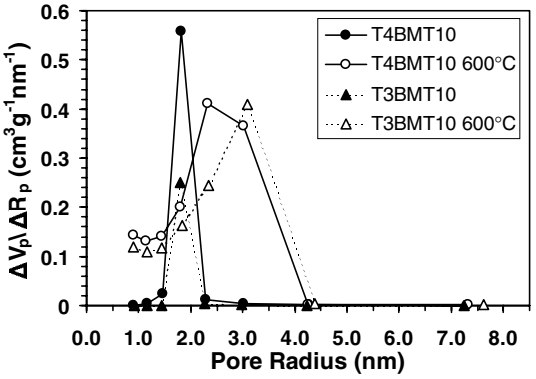

Figure 18. Comparison of pore radius distributions in hybrids T4BMT10 and T3BMT10 (filled symbols) with those in ashes (open symbols) originated from respective hybrids after heating to 600°C.

3.7. Heat-Treated Samples

To evaluate changes in pore structure upon polymer elimination, hybrids TxBMT10 were heat treated to 600°C. Figure 17 compares the results for pore radius and pore volume of the treated samples, which will be referred as hybrid ashes, with those of the original hybrids. In a general manner, it can be observed that pore volume and size of ashes follow the same tendency as for hybrids, decreasing with increasing polymer content. As expected, pore volumes of ashes are larger than those of the original hybrids due to polymer elimination. It is also observed that the difference between pore volumes in ashes and in respective hybrids increase with increasing polymer content, which is a mere consequence of the larger volumes occupied by polymer in the hybrids.

Pores arising from polymer degradation must correspond to either the places where polymer molecules were lodged or the pores that were obstructed by them. According to the literature [31, 32], the thermal treatment at 600°C would not affect silica network morphology and the resulting pore size would correspond to the size of polymeric domains in the hybrid structure. Figure 17 shows that the average pore radii are always smaller in ashes than in the correspondent hybrids. However, Fig. 18, which compares pore radius distributions in hybrids T4BMT10 and T3BMT10 with those in their respective ashes, demonstrates that micro and mesopores have arisen after polymer degradation. The occurrence of micropores as in silica (Fig. 14) suggests that they were already present in original hybrids, but inaccessible to N_2 molecules. The appearance of

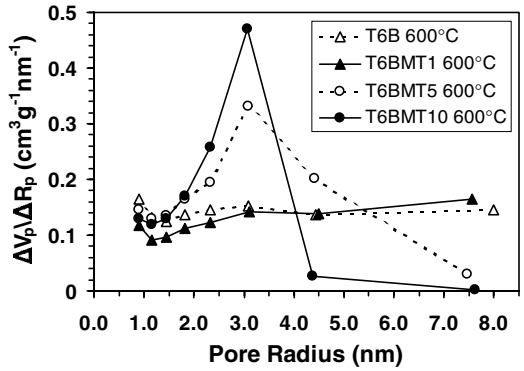

Figure 19. Comparison of pore radius distributions in ashes originated after heating to 600°C hybrids T6BMTy with increasing bonding agent content.

mesopores in the range of 2 nm to 4 nm (4 nm to 8 nm in diameter) means that polymeric domains in hybrids TxBMT10 are dispersed at the nanometric scale.

Figure 19 compares pore radius distributions in ashes originated from hybrids T6BMTy with different bonding agent contents. It can be observed that, while the distributions for ashes obtained from hybrids T6B and T6BMT1 are considerably broad, an evident narrowing occurs when bonding agent content in original hybrids is increased, until a definite peak appears at ∼3.0 nm in ashes T6BMT10. These results imply that the mean size of polymeric domains in the hybrid structure becomes smaller with progressively larger bonding agent contents. This fact demonstrates that, even though interactions between PBA segments and silica are unfavorable, the addition of MPTS contributes significantly to improve homogeneity of hybrid structure due to an

intimate interpenetration of polymer chains within silica network.

4. Conclusions

Porous sol-gel derived PBA-silica hybrids obtained with similar polymer contents and different MPTS contents exhibited distinct structures. Pore volumes, pore sizes and particle sizes were progressively increased with decreasing bonding agent or solvent contents. These results imply that condensation of PBA-silica particles is hindered by hydrophobic PBA domains in a more heterogeneous medium, causing an inefficient packing of hybrid particles. The formation of primary bonds between PBA segments and silica network is an effective way of reducing size of polymeric domains and producing a more homogeneous structure with smaller uniform-sized pores. There is evidence for the presence of ink bottle pores with extremely narrow throat size distribution in hybrids with larger polymer and bonding agent contents, which may be useful for certain technological applications involving molecular size selectivity.

Acknowledgments

The authors gratefully acknowledge FAPEMIG, CNPq and CAPES for the financial support. RORC also thanks Max P. Ferreira (CDTN), for gently offering his lab for partial development of this study, and Ney P. Sampaio (Dept. of Physics—UFMG), for his kind collaboration on acquirement of SEM images.

References

1. D.A. Loy, MRS Bull. **26**, 364 (2001).
2. C.J. Brinker and G.W. Scherer, *Sol-Gel Science: The Physics and Chemistry of Sol-Gel Processing* (Academic Press, San Diego, 1990), pp. 465, 524.
3. J.E. Mark, C.Y. Jiang, and M.Y. Tang, Macromolecules **17**, 2613 (1984).
4. H.H. Huang, B. Orler, and G.L. Wilkes, Polym. Bull. **14**, 557 (1985).
5. E.J.A. Pope, M. Asami, and J.D. Mackenzie, J. Mater. Res. **4**, 1018 (1989).
6. B.M. Novak, Adv. Mater. **5**, 442 (1993).
7. L. Mascia, Trends Polym. Sci. **3**, 61 (1995).
8. A.B. Brennan and T.M. Miller, in *Kirk-Othmer Encyclopedia of Chemical Technology*, 4 ed. (Wiley, New York, 1994), Vol. 12, p. 644.
9. J. Wen and G.L. Wilkes, Chem. Mater. **8**, 1667 (1996).
10. P. Judeinstein and C. Sanchez, J. Mater. Chem. **6**, 511 (1996).
11. A.B. Wojcik and L.C. Klein, Appl. Organometal. Chem. **11**, 129 (1997).
12. Y. Chujo and R. Tamaki, MRS Bull. **26**, 389 (2001).
13. C.J. Brinker, Curr. Opin. Solid Mater. Sci. **1**, 798 (1996).
14. A. Stein, Micropor. Mesopor. Mater. **44–55**, 227 (2001).
15. B. Lindlar, A. Kogelbauer, P.J. Kooyman, and R. Prins, Micropor. Mesopor. Mater. **44–55**, 89 (2001).
16. Y. Lu, G. Cao, R.P. Kale, S. Prabakar, G.P. López, and C.J. Brinker, Chem. Mater. **11**, 1223 (1999).
17. C. Yu, Y. Yu, L. Miao, and D. Zhao, Micropor. Mesopor. Mater. **44–55**, 65 (2001).
18. K.A. Mauritz and C.K. Jones, J. Appl. Polym. Sci. **40**, 1401 (1990).
19. M. Motomatsu, T. Takahashi, H.Y. Nie, W. Mizutani, and H. Tokumoto, Polymer **38**, 177 (1997).
20. W. Zhou, J.H. Dong, K.Y. Qiu, and Y. Wei, J. Appl. Polym. Sci. **73**, 419 (1999).
21. C.K. Chan, I.M. Chu, W. Lee, and W.K. Chin, Macromol. Chem. Phys. **22**, 911 (2001).
22. S.J. Gregg and K.S.W. Sing, *Adsorption, Surface Area and Porosity*, 2 ed. (Academic Press, San Diego, 1982).
23. P.A. Webb and C. Orr, *Analytical Methods on Fine Particle Technology* (Micromeritcs Instrument Corporation, Norcross, 1997).
24. P. Bosch, F. Monte, J.L. Mateo, and D. Levy, J. Polym. Sci. A: Polym. Chem. **34**, 3289 (1996).
25. Z.H. Huang and K.Y. Qiu, Polymer **38**, 521 (1997).
26. R.O.R. Costa and W.L. Vasconcelos, J. Non-Cryst. Sol. **304**, 84 (2002).
27. I.K. Varma, A.K. Tomar, and R.C. Anand, J. Appl. Polym. Sci. **33**, 1377 (1987).
28. S. Yano, K. Nakamura, M. Kodomari, and N. Yanauchi, J. Appl. Polym. Sci. **54**, 163 (1994).
29. J.C. Pouxviel, J.P. Boilet, J.C. Beloeil, and J.Y. Allemand, J. Non-Cryst. Sol. **89**, 345 (1987).
30. R.O.R. Costa, W.L. Vasconcelos, and F.S. Lameiras, J. Mater. Sci., submitted.
31. T. Saegusa, J. Macromol. Sci.-Chem. **A28**, 817 (1991).
32. R. Tamaki and Y. Chujo, Appl. Organomet. Chem. **12**, 775 (1998).